

## Extended formulation of isotropic hardening stagnation behavior in cyclic loading of metals by the subloading surface model

Koichi Hashiguchi\* and Toshiyuki Ozaki\*\*

\* Member Dr. of Eng. and Dr. of Agr., Prof., Dept. Civil and Environ. Eng.,  
College of Technology, Daiichi University,  
(Kokubu-Chuo 1-10-2, Kirishima-shi, Kagoshima-ken 899-4395, Japan)

\*\* Member Dr. of Agr., Manager of Transmission Line Engineering Dept. Kyushu Electric Engineering  
Consultants Inc. (Kyuken-Bld.7F, Kiyokawa 2-13-6, Chuo-ku, Fukuoka, 810-0005, Japan)

The stagnation phenomenon of isotropic hardening is observed in the cyclic loading behavior of metals. An extended formulation of this phenomenon is formulated so as to describe the smooth evolution of isotropic hardening by incorporating the concept of the subloading surface, which falls within the framework of stress space formulation. In addition it is furnished with the controlling function of the isotropic hardening stagnation variable and thus it does not require any return-mapping algorithm.

*Key Words:* constitutive equation, elastoplasticity, metals, isotropic hardening stagnation, subloading surface model, viscoplasticity

### 1. Introduction

The isotropic hardening of metals is induced by the equivalent plastic strain. It is observed in experiments for the deformation behavior of various metals that the isotropic hardening stagnates despite of development in the equivalent plastic strain for a certain range in the initial stage of re-yielding after the reverse loading. This phenomenon influences remarkably the cyclic loading behavior in which the reverse deformations are repeated. In order to describe this phenomenon the idea of the nonhardening region postulating that the isotropic hardening stagnates when the plastic strain exists in a certain region in the plastic strain space was proposed by Chaboche et al.<sup>1)</sup> (see also Lemaitre and Chaboche<sup>2)</sup> and improved by Ohno<sup>3)</sup> and Ohno and Kachi<sup>4)</sup>. It is similar to the concept of yield surface assuming that the plastic strain is induced when the stress reaches it. However, the accumulation of plastic strain rate has not any physical meaning except for the case that the principal axes of plastic strain rate are fixed. Further, needless to say, the movement of nonhardening region cannot be shown in the stress space and thus it has to be demonstrated separately from the yield surface. Further, It was modified by Yoshida and Uemori<sup>5),6)</sup> into the stress space formulation as the isotropic hardening stagnates when the back stress exists in the certain region of stress

space. However, it cannot describe the stagnation behavior of isotropic hardening in materials without the kinematic hardening. In these formulations, the isotropic hardening is induced suddenly when the plastic strain or the back stress reaches the isotropic hardening surface violating the smoothness condition<sup>7)-10)</sup>. Then, Hashiguchi and Yoshimaru<sup>11)</sup> improved these formulations of Chaboche and Ohno so as to describe the smooth development of isotropic hardening by incorporating the concept of subloading surface.

A pertinent formulation of isotropic stagnation behavior is given below by incorporating the concept of the subloading surface falling within the framework of stress space formulation and is free from the kinematic hardening. It is capable of describing the smooth evolution of isotropic hardening. In addition it is furnished with the controlling function of the isotropic hardening stagnation variable and thus it does not require any return-mapping algorithm.

### 2. Strain rates and volumetric strains

Denoting the current configuration of the material particle as  $x$  and the current velocity as  $v$ , the velocity gradient is de-

scribed as  $\mathbf{L} = \partial \mathbf{v} / \partial \mathbf{x}$ . The strain rate and the continuum spin are defined as  $\mathbf{D} \equiv (\mathbf{L} + \mathbf{L}^T) / 2$  and  $\mathbf{W} \equiv (\mathbf{L} - \mathbf{L}^T) / 2$ , respectively,  $( )^T$  standing for the transpose. Limiting to the infinitesimal strain, let the strain rate  $\mathbf{D}$  be additively decomposed into the elastic strain rate  $\mathbf{D}^e$  and the plastic strain rate  $\mathbf{D}^p$  as follows:

$$\mathbf{D} = \mathbf{D}^e + \mathbf{D}^p \quad (1)$$

where  $\mathbf{D}^e$  is related linearly to the stress rate as follows:

$$\mathbf{D}^e = \mathbf{E}^{-1} \overset{\circ}{\boldsymbol{\sigma}} \quad (2)$$

where  $\mathbf{E}$  is the fourth-order elastic stiffness tensor, and  $\boldsymbol{\sigma}$  is the Cauchy stress.  $(\overset{\circ}{\phantom{x}})$  denotes the proper objective corotational rate.

### 3. Extended subloading surface model for metals

The extended subloading surface model specialized for metals is formulated below.

The following yield surface with the isotropic-kinematic combined hardening is assumed.

$$f(\hat{\boldsymbol{\sigma}}) = F(H) \quad (3)$$

where

$$\hat{\boldsymbol{\sigma}} \equiv \boldsymbol{\sigma} - \boldsymbol{\alpha} \quad (4)$$

$H$  is the isotropic hardening variable and  $\boldsymbol{\alpha}$  ( $\text{tr} \boldsymbol{\alpha} = 0$ ) is the back stress. Here, for sake of simplicity in formulation it let be assumed that  $f(\hat{\boldsymbol{\sigma}})$  is the homogeneous function of  $\hat{\boldsymbol{\sigma}}$  in degree-one. Therefore, it holds that

$$f(s\hat{\boldsymbol{\sigma}}) = sf(\hat{\boldsymbol{\sigma}}) \quad (5)$$

$$\text{tr} \left( \frac{\partial f(\hat{\boldsymbol{\sigma}})}{\partial \hat{\boldsymbol{\sigma}}} \hat{\boldsymbol{\sigma}} \right) = f(\hat{\boldsymbol{\sigma}}) \quad (6)$$

where  $s$  is an arbitrary positive scalar quantity and  $\text{tr}(\phantom{x})$  designates the trace, whilst Eq. (6) is based on the Euler's homogeneous function of degree-one. Therefore, the yield surface of Eq. (3) keeps the similar shape and orientation with respect to  $\boldsymbol{\alpha}$ .

Here, let the following evolution rule of the internal variables be given as follows:

$$\dot{\boldsymbol{\alpha}} = \mathbf{a}(\boldsymbol{\sigma}, H_i) \|\mathbf{D}^p\|, \quad \dot{H} = h(\boldsymbol{\sigma}, H_i, \mathbf{D}^p) \quad (7)$$

where  $H_i$  ( $i = 1, 2, \dots$ ) stands for scalar- or tensor-valued internal variables collectively. The scalar function  $h$  has to be the homogeneous degree one in  $\mathbf{D}^p$  since the rate-independent behavior is considered in the present formulation, fulfilling  $h(\boldsymbol{\sigma}, H_i, s\mathbf{D}^p) = sh(\boldsymbol{\sigma}, H_i, \mathbf{D}^p)$ .

In what follows, we introduce the *subloading surface model* as the unconventional plasticity model in which it is assumed that the interior of the yield surface is not a purely elastic domain but the plastic strain rate is induced by the rate of stress inside that surface. Here, let it be assumed that the plastic strain rate develops

gradually as the stress approaches the yield surface and let the subloading surface be introduced in order to describe the degree of approach to the yield surface, which always passes through the current stress point  $\boldsymbol{\sigma}$  and keeps a similar shape and orientation to the normal-yield surface. Then, let the yield surface be renamed as the *normal sliding-yield surface*.

The subloading surface fulfills the following geometrical characteristics.

- i) All lines connecting an arbitrary point inside the subloading surface and its conjugate point inside the normal-yield surface join at a unique point, called the *similarity center*.
- ii) All ratios of length of an arbitrary line-element connecting two points inside the subloading surface to that of an arbitrary conjugate line-element connecting two conjugate points inside the normal-yield surface are identical. The ratio is called the *similarity ratio*, which coincides with the ratio of the sizes of these surfaces.

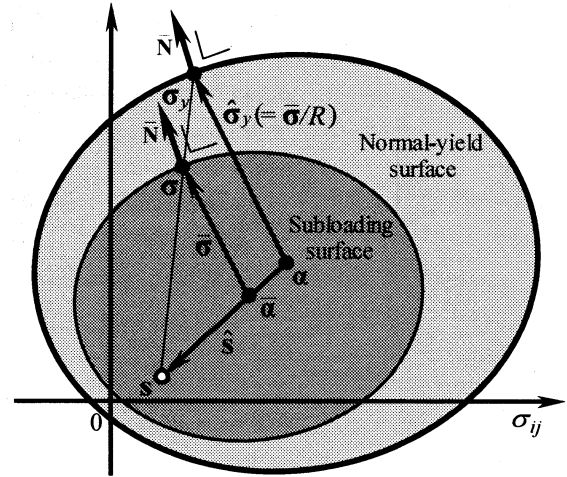


Fig. 1. Normal-yield and subloading surfaces.

Let the similarity ratio in the subloading surface model be called specifically the *normal-yield ratio*, denoted by  $R$  ( $0 \leq R \leq 1$ ), where  $R = 0$  corresponds to the null traction state ( $f = 0$ ) as the most elastic state,  $0 < R < 1$  to the *subyield state* ( $0 < f < F$ ), and  $R = 1$  to the *normal-yield state* in which the stress lies on the normal sliding-yield surface ( $f = F$ ). Therefore, the normal-yield ratio  $R$  plays the role of three-dimensional measure of the degree of approach to the normal-yield state. Then, the subloading surface is described by

$$f(\bar{\boldsymbol{\sigma}}) = RF(H) \quad (8)$$

where

$$\bar{\boldsymbol{\sigma}} \equiv \boldsymbol{\sigma} - \bar{\boldsymbol{\alpha}} \quad (9)$$

$\bar{\boldsymbol{\alpha}}$  in the subloading surface is the conjugate point of  $\boldsymbol{\alpha}$  in the normal-yield surface (Fig. 1). Denoting the similarity center be denoted by  $\mathbf{s}$  and the conjugate point on the normal-yield surface

to the current stress point  $\boldsymbol{\sigma}$  by  $\boldsymbol{\sigma}_y$ , it can be written as

$$\bar{\boldsymbol{\sigma}} = R \hat{\boldsymbol{\sigma}}_y \quad (10)$$

$$\bar{\mathbf{s}} = R \hat{\mathbf{s}}, \quad \bar{\boldsymbol{\alpha}} = \mathbf{s} - R \hat{\mathbf{s}} \quad (11)$$

where

$$\hat{\boldsymbol{\sigma}}_y \equiv \boldsymbol{\sigma}_y - \boldsymbol{\alpha}, \quad \bar{\boldsymbol{\sigma}} \equiv \boldsymbol{\sigma} - \bar{\boldsymbol{\alpha}} \quad (12)$$

$$\hat{\mathbf{s}} \equiv \mathbf{s} - \boldsymbol{\alpha}, \quad \bar{\mathbf{s}} \equiv \mathbf{s} - \bar{\boldsymbol{\alpha}} \quad (13)$$

Further, it holds from Eqs. (11) and (13)<sub>2</sub> that

$$\bar{\boldsymbol{\sigma}} \equiv \tilde{\boldsymbol{\sigma}} + R \hat{\mathbf{s}} \quad (14)$$

where

$$\tilde{\boldsymbol{\sigma}} \equiv \boldsymbol{\sigma} - \mathbf{s} \quad (15)$$

$R$  is the ratio of the size of the subloading surface to that of the normal-yield surface,  $\mathbf{s}$  is the similarity-center of the normal-yield and the subloading surfaces, and  $\bar{\boldsymbol{\alpha}}$  is the conjugate point on the subloading surface to the point  $\boldsymbol{\alpha}$  on the normal-yield surface.

By substituting Eq. (14) into Eq. (8), the subloading surface is rewritten as

$$f(\tilde{\boldsymbol{\sigma}} + R \hat{\mathbf{s}}) = RF(H) \quad (16)$$

The values of  $R$  is calculated from Eq. (16) by substituting the known values  $\boldsymbol{\sigma}, \mathbf{s}, \boldsymbol{\alpha}, H$ , while the numerical calculation is required in general.

The material-time derivative of Eq. (8) is given as

$$\text{tr}\left(\frac{\partial f(\bar{\boldsymbol{\sigma}})}{\partial \bar{\boldsymbol{\sigma}}}\dot{\bar{\boldsymbol{\sigma}}}\right) - \text{tr}\left(\frac{\partial f(\bar{\boldsymbol{\sigma}})}{\partial \bar{\boldsymbol{\sigma}}}\dot{\bar{\boldsymbol{\alpha}}}\right) = \dot{R}F + RF\dot{H} \quad (17)$$

where

$$F' \equiv dF/dH \quad (18)$$

Eq. (17) is rewritten as

$$\text{tr}(\bar{\mathbf{N}}\dot{\bar{\boldsymbol{\sigma}}}) - \text{tr}(\bar{\mathbf{N}}\dot{\bar{\boldsymbol{\alpha}}}) = \left(\frac{\dot{R}}{R} + \frac{F'}{F}\dot{H}\right)\text{tr}(\bar{\mathbf{N}}\bar{\boldsymbol{\sigma}}) \quad (19)$$

where

$$\bar{\mathbf{N}} \equiv \frac{\partial f(\bar{\boldsymbol{\sigma}})}{\partial \bar{\boldsymbol{\sigma}}} / \left\| \frac{\partial f(\bar{\boldsymbol{\sigma}})}{\partial \bar{\boldsymbol{\sigma}}} \right\| \quad (\|\bar{\mathbf{N}}\| = 1) \quad (20)$$

noting the following relation due to the Euler's homogeneous function of degree-one.

$$\frac{\partial f(\bar{\boldsymbol{\sigma}})}{\partial \bar{\boldsymbol{\sigma}}} = \frac{\text{tr}\left(\frac{\partial f(\bar{\boldsymbol{\sigma}})}{\partial \bar{\boldsymbol{\sigma}}}\bar{\boldsymbol{\sigma}}\right)}{\text{tr}(\bar{\mathbf{N}}\bar{\boldsymbol{\sigma}})}\bar{\mathbf{N}} = \frac{f(\bar{\boldsymbol{\sigma}})}{\text{tr}(\bar{\mathbf{N}}\bar{\boldsymbol{\sigma}})}\bar{\mathbf{N}} = \frac{RF}{\text{tr}(\bar{\mathbf{N}}\bar{\boldsymbol{\sigma}})}\bar{\mathbf{N}} \quad (21)$$

The direct transformation of the material-time derivative to the corotational derivative is verified for the general scalar function<sup>12</sup>.

From Eq. (11)<sub>2</sub>  $\dot{\bar{\boldsymbol{\alpha}}}$  is expressed as follows:

$$\dot{\bar{\boldsymbol{\alpha}}} = R\dot{\boldsymbol{\alpha}} - \dot{R}\hat{\mathbf{s}} + (1-R)\dot{\hat{\mathbf{s}}} \quad (22)$$

The substitution of Eq. (22) into Eq. (19) leads to

$$\begin{aligned} \text{tr}(\bar{\mathbf{N}}\dot{\bar{\boldsymbol{\sigma}}}) - \text{tr}[\bar{\mathbf{N}}\{\dot{R}\hat{\boldsymbol{\alpha}} - \dot{R}\hat{\mathbf{s}} + (1-R)\dot{\hat{\mathbf{s}}}\}] \\ = \left(\frac{\dot{R}}{R} + \frac{F'}{F}\dot{H}\right)\text{tr}(\bar{\mathbf{N}}\bar{\boldsymbol{\sigma}}) \end{aligned} \quad (23)$$

As observed in experiments, the stress asymptotically approaches the normal-yield surface in the plastic loading process  $\mathbf{D}^p \neq \mathbf{0}$ . Thus, the following evolution equation of the normal-yield ratio  $R$  is assumed (see Fig. 2).

$$\dot{R} = U\|\mathbf{D}^p\| \quad \text{for } \mathbf{D}^p \neq \mathbf{0} \quad (24)$$

where  $U$  is a monotonically decreasing function of the normal-yield ratio  $R$ , fulfilling

$$U(R) \begin{cases} \rightarrow +\infty & \text{for } 0 \leq R \leq R_e \text{ (almost elastic state)} \\ > 0 & \text{for } R_e < R < 1 \text{ (sub-yield state),} \\ = 0 & \text{for } R = 1 \text{ (normal-yield state),} \\ < 0 & \text{for } R > 1 \text{ (over-yield state)} \end{cases} \quad (25)$$

$R_e (< 1)$  is the material constant describing the elastic limit of  $R$ , whilst  $R_e \geq 0.5$  for many metals. Let the function  $U$  satisfying Eq. (25) be simply given by

$$U(R) = u \cot\left(\frac{\pi}{2} \frac{\langle R - R_e \rangle}{1 - R_e}\right) \quad (26)$$

where  $u$  is the material constant. The symbol  $\langle \cdot \rangle$  is the McCauley's bracket, i.e.  $\langle s \rangle = (s + |s|)/2$  for an arbitrary scalar variable  $s$ .

Eq. (24) with Eq. (26) can lead to the analytical integration of  $R$  for the accumulated plastic strain  $\varepsilon^p \equiv \int \|\mathbf{D}^p\| dt$  under the initial condition  $R = R_0: \varepsilon^p = \varepsilon_0^p$  as follows:

$$R = \frac{2}{\pi}(1 - R_e)\cos^{-1}\left\{\cos\left(\frac{\pi}{2}\frac{R_0 - R_e}{1 - R_e}\right)\exp\left(-\frac{\pi}{2}u\frac{\varepsilon^p - \varepsilon_0^p}{1 - R_e}\right)\right\} + R_e \quad (27)$$

On the other hand, the following function has been used widely so far.

$$U(R) = -u \ln \frac{\langle R - R_e \rangle}{1 - R_e} \quad (28)$$

However, an analytical integration cannot be obtained from Eq. (24) with Eq. (28) and thus Eq. (28) is inconvenient to formulate the return-mapping method attracting the stress to the subloading surface<sup>13</sup>. By adopting the following function for  $u$  the stress-strain curve is modified such that the stress returns quickly to the monotonic loading curve in the reloading process after the unloading.

$$u(\tilde{R}) = \frac{u_a}{\exp(u_b \tilde{R})} \quad (29)$$

where  $u_a$  and  $u_b$  are the material constants.

The evolution rule of the similarity center is given as follows<sup>14</sup>:

$$\dot{\hat{\mathbf{s}}} = c\|\mathbf{D}^p\|\frac{\tilde{\boldsymbol{\sigma}}}{R} + \dot{\boldsymbol{\alpha}} + \frac{\dot{F}}{F}\hat{\mathbf{s}} \quad (30)$$

The substitution of Eq. (30) into Eq. (23) leads to

$$\begin{aligned} \text{tr}(\bar{\mathbf{N}} \dot{\bar{\boldsymbol{\sigma}}}) - \text{tr} \left[ \bar{\mathbf{N}} \left\{ R \dot{\bar{\boldsymbol{\alpha}}} - \dot{R} \hat{\mathbf{s}} + (1-R) \left( c \|\mathbf{D}^p\| \frac{\tilde{\boldsymbol{\sigma}}}{R} + \dot{\bar{\boldsymbol{\alpha}}} + \frac{F'}{F} \hat{\mathbf{s}} \right) \right\} \right] \\ = \left( \frac{\dot{R}}{R} + \frac{F'}{F} \dot{H} \right) \text{tr}(\bar{\mathbf{N}} \bar{\boldsymbol{\sigma}}) \end{aligned} \quad (31)$$

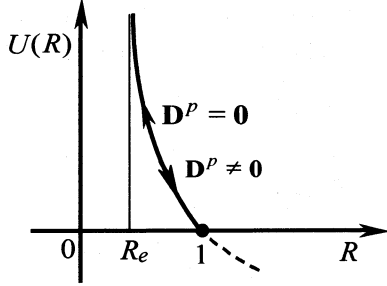


Fig. 2. Function  $U(R)$  in evolution rule of normal-yield ratio.

which is rewritten as

$$\begin{aligned} \text{tr}(\bar{\mathbf{N}} \dot{\bar{\boldsymbol{\sigma}}}) - \text{tr} \left[ \bar{\mathbf{N}} \left\{ \frac{F'}{F} \dot{H} \left\{ (1-R) \hat{\mathbf{s}} + \bar{\boldsymbol{\sigma}} \right\} + \dot{\bar{\boldsymbol{\alpha}}} \right. \right. \\ \left. \left. + \left\{ \dot{R} \left( \frac{1}{R} \bar{\boldsymbol{\sigma}} - \hat{\mathbf{s}} \right) + c \left( \frac{1}{R} - 1 \right) \|\mathbf{D}^p\| \tilde{\boldsymbol{\sigma}} \right\} \right\} \right] = 0 \end{aligned} \quad (32)$$

The substitution of

$$\left. \begin{aligned} (1-R) \hat{\mathbf{s}} + \bar{\boldsymbol{\sigma}} &= \mathbf{s} - \bar{\boldsymbol{\alpha}} - (\mathbf{s} - \bar{\boldsymbol{\alpha}}) + \bar{\boldsymbol{\sigma}} - \bar{\boldsymbol{\alpha}} = \hat{\boldsymbol{\sigma}} \\ \frac{1}{R} \bar{\boldsymbol{\sigma}} - \hat{\mathbf{s}} &= \frac{\tilde{\boldsymbol{\sigma}} + R \hat{\mathbf{s}}}{R} - \hat{\mathbf{s}} = \frac{\tilde{\boldsymbol{\sigma}}}{R} \end{aligned} \right\} \quad (33)$$

due to Eqs. (9), (11), (13) and (14) into Eq. Eqs. (32) leads to

$$\begin{aligned} \text{tr}(\bar{\mathbf{N}} \dot{\bar{\boldsymbol{\sigma}}}) - \text{tr} \left[ \bar{\mathbf{N}} \left\{ \frac{F'}{F} \dot{H} \hat{\boldsymbol{\sigma}} + \dot{\bar{\boldsymbol{\alpha}}} \right. \right. \\ \left. \left. + \left\{ \dot{R} \frac{\tilde{\boldsymbol{\sigma}}}{R} + c \left( \frac{1}{R} - 1 \right) \|\mathbf{D}^p\| \tilde{\boldsymbol{\sigma}} \right\} \right\} \right] = 0 \end{aligned} \quad (34)$$

Substituting Eqs. (7) and (24) into Eq. (34), one has the *consistency condition* for the subloading surface model:

$$\begin{aligned} \text{tr}(\bar{\mathbf{N}} \dot{\bar{\boldsymbol{\sigma}}}) - \text{tr} \left[ \bar{\mathbf{N}} \left\{ \frac{F'}{F} h(\boldsymbol{\sigma}, H_i, \mathbf{D}^p) \hat{\boldsymbol{\sigma}} + \mathbf{a}(\boldsymbol{\sigma}, H_i) \|\mathbf{D}^p\| \right. \right. \\ \left. \left. + \left\{ \frac{U}{R} + c \left( \frac{1}{R} - 1 \right) \right\} \|\mathbf{D}^p\| \tilde{\boldsymbol{\sigma}} \right\} \right] = 0 \end{aligned} \quad (35)$$

Substituting the plastic flow rule

$$\mathbf{D}^p = \bar{\lambda} \bar{\mathbf{N}} \quad (\bar{\lambda} > 0) \quad (36)$$

into Eq. (35), the proportionality factor  $\bar{\lambda}$  is derived as

$$\bar{\lambda} = \frac{\text{tr}(\bar{\mathbf{N}} \dot{\bar{\boldsymbol{\sigma}}})}{\bar{M}^p}, \quad \mathbf{D}^p = \frac{\text{tr}(\bar{\mathbf{N}} \dot{\bar{\boldsymbol{\sigma}}})}{\bar{M}^p} \bar{\mathbf{N}} \quad (37)$$

where the plastic modulus  $\bar{M}^p$  is given as

$$\bar{M}^p \equiv \text{tr} \left[ \bar{\mathbf{N}} \left\{ \frac{F'}{F} h(\boldsymbol{\sigma}, H_i, \bar{\mathbf{N}}) \hat{\boldsymbol{\sigma}} + \mathbf{a}(\boldsymbol{\sigma}, H_i) \right\} \right]$$

$$+ \left\{ \frac{U}{R} + c \left( \frac{1}{R} - 1 \right) \right\} \tilde{\boldsymbol{\sigma}} \right] \quad (38)$$

Substituting Eqs. (2) and (37) into Eq. (1), the strain rate is given by

$$\mathbf{D} = \mathbf{E}^{-1} \dot{\bar{\boldsymbol{\sigma}}} + \frac{\text{tr}(\bar{\mathbf{N}} \dot{\bar{\boldsymbol{\sigma}}})}{\bar{M}^p} \bar{\mathbf{N}} \quad (39)$$

from which the positive proportionality factor  $\bar{\lambda}$  described in terms of strain rate is derived as

$$\bar{\lambda} = \frac{\text{tr}(\bar{\mathbf{N}} \mathbf{E} \mathbf{D})}{\bar{M}^p + \text{tr}(\bar{\mathbf{N}} \mathbf{E} \bar{\mathbf{N}})}, \quad \mathbf{D}^p = \frac{\text{tr}(\bar{\mathbf{N}} \mathbf{E} \mathbf{D})}{\bar{M}^p + \text{tr}(\bar{\mathbf{N}} \mathbf{E} \bar{\mathbf{N}})} \bar{\mathbf{N}} \quad (40)$$

The stress rate is given from Eqs. (1), (2) and (40) as

$$\dot{\bar{\boldsymbol{\sigma}}} = \mathbf{E} \mathbf{D} - \frac{\text{tr}(\bar{\mathbf{N}} \mathbf{E} \mathbf{D})}{\bar{M}^p + \text{tr}(\bar{\mathbf{N}} \mathbf{E} \bar{\mathbf{N}})} \mathbf{E} \bar{\mathbf{N}} \quad (41)$$

The loading criterion is given as follows<sup>15), 10)</sup>:

$$\left. \begin{aligned} \mathbf{D}^p \neq \mathbf{0} : \bar{\lambda} \text{ or } \bar{\lambda} > 0, \\ \mathbf{D}^p = \mathbf{0} : \text{otherwise} \end{aligned} \right\} \quad (42)$$

#### 4. Cyclic stagnation of isotropic hardening

First, introduce the novel variable  $\xi$  ( $\text{tr} \xi = 0$ ), called the *isotropic hardening stress*, which translates in the direction of the plastic strain rate so that the evolution rule is given by

$$\dot{\xi} = \xi_{\sigma} \mathbf{D}^p = \xi_{\sigma} \|\mathbf{D}^p\| \bar{\mathbf{N}} \quad (43)$$

where  $\xi_{\sigma}$  ( $\geq 0$ ) is the positive variable having the dimension of stress, which will be formulated later.

Then, incorporate the *normal-isotropic hardening surface* which regulates the isotropic hardening so as to stagnate when the isotropic hardening stress  $\xi$  lies inside this surface, and let it be described by

$$f(\xi) = \mu F(H) \quad (44)$$

where  $\mu$  ( $< 1$ ) is the material constant and

$$\xi \equiv \xi - \bar{\boldsymbol{\alpha}} \quad (45)$$

$\bar{\boldsymbol{\alpha}}$  is the center of the normal-isotropic hardening surface, the evolution rule of which will be given later.

Further, incorporate the surface, called the *sub-isotropic hardening surface* (Fig. 3) which always passes through the current point  $\xi$  and has the similar shape and orientation to the normal-isotropic hardening surface. Then, it is mathematically expressed as

$$f(\check{\xi}) = \check{R} \mu F(H) \quad (46)$$

where  $\check{R}$  ( $0 \leq \check{R} \leq 1$ ) is the ratio of the size of sub-isotropic hardening surface to that of the nor-

mal-isotropic hardening surface and thus it plays the role as the measure to describe the approaching degree of  $\xi$  to the normal-isotropic hardening surface. Then,  $\bar{R}$  is called the *normal-isotropic hardening ratio*. It is calculated from the equation  $\bar{R} = f(\xi)/K$  in terms of the known values  $f(\xi)$  and  $K$ .

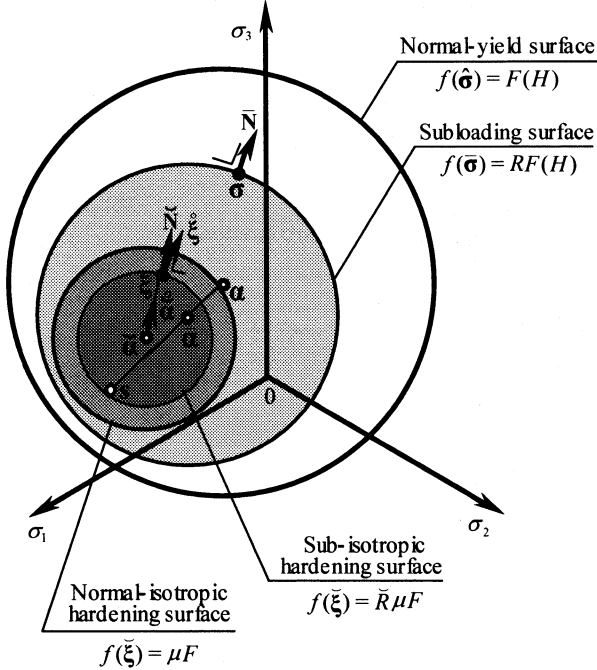


Fig. 3. Normal- and sub-isotropic hardening surfaces.

The material-time derivative of Eq. (46) leads to

$$\text{tr} \left( \frac{\partial f(\xi)}{\partial \xi} \dot{\xi} \right) - \text{tr} \left( \frac{\partial f(\xi)}{\partial \xi} \dot{\alpha} \right) = \bar{R} \mu \dot{F} + \dot{\bar{R}} \mu F \quad (47)$$

which is rewritten as

$$\text{tr}(\bar{N} \dot{\xi}) - \text{tr}(\bar{N} \dot{\alpha}) = \mu \left( \bar{R} \frac{F'}{F} \dot{H} + \frac{\dot{\bar{R}}}{\bar{R}} \right) \text{tr}(\bar{N} \xi) \quad (48)$$

by use of the Euler's theorem for the homogeneous function of  $\xi$  in degree-one, i.e.

$$\frac{\partial f(\xi)}{\partial \xi} = \frac{\text{tr} \left( \frac{\partial f(\xi)}{\partial \xi} \xi \right)}{\text{tr}(\bar{N} \xi)} = \frac{f(\xi)}{\text{tr}(\bar{N} \xi)} = \frac{\bar{R} F}{\text{tr}(\bar{N} \xi)}$$

where

$$\bar{N} = \frac{\partial f(\xi)}{\partial \xi} / \left\| \frac{\partial f(\xi)}{\partial \xi} \right\| \quad (49)$$

Now, it is assumed that the isotropic hardening variable evolves under the conditions:

- 1) The isotropic hardening is induced when the plastic strain rate is directed the outward of the sub-isotropic hardening surface.

- 2) The isotropic hardening develops as the isotropic hardening stress  $\xi$  approaches the normal-isotropic hardening surface so that the normal-hardening ratio increases.
- 3) The isotropic hardening variable evolves by the rule (7)<sub>2</sub> when the normal-isotropic hardening ratio is unity, i.e. the isotropic hardening stress  $\xi$  lies on the normal-isotropic hardening surface.

Then, let the following evolution rule of isotropic hardening be assumed by extending Eq. (7)<sub>2</sub>.

$$\dot{H} = h(\sigma, H_i, \bar{R}^\nu \langle \text{tr}(\bar{N} \mathbf{D}^p) \rangle) \quad (50)$$

where  $\nu (\geq 1)$  is the material constant.

Next, let it be assumed that the center of normal-isotropic hardening surface evolves in the following manner:

- 1) The center of normal-isotropic hardening surface moves when the plastic strain rate is directed the outward of the sub-isotropic hardening surface.
- 2) The movement of the center of normal-isotropic hardening surface develops as the isotropic hardening stress  $\xi$  approaches the normal-isotropic hardening surface in the identical manner as the isotropic hardening variable.
- 3) The center of normal-isotropic hardening surface translates in the direction of the outer-normal of the sub-isotropic hardening surface at the current isotropic hardening stress.

Then, let the following evolution rule for the center of the normal-isotropic hardening surface be assumed

$$\dot{\alpha} = \bar{a} \bar{R}^\nu \langle \text{tr}(\bar{N} \mathbf{D}^p) \rangle \bar{N} = \bar{a} \bar{R}^\nu \|\mathbf{D}^p\| \langle \text{tr}(\bar{N} \bar{N}) \rangle \bar{N} \quad (51)$$

where  $\bar{a}$  is the material constant (or material function of stress in general) having the dimension of stress.

Next, let it be assumed that the normal-isotropic hardening ratio increases under the conditions:

- 1) The normal-isotropic hardening ratio increases when the plastic strain rate is directed the outward of the sub-isotropic hardening surface.
- 2) The normal-isotropic hardening ratio increases infinitely without change of the normal-isotropic hardening surface when it is zero but it increases no more when it reaches unity, i.e. when  $\xi$  reaches the normal-isotropic hardening surface.

Then, let the following evolution rule of the normal-isotropic hardening ratio be assumed.

$$\dot{\bar{R}} = \bar{U}(\bar{R}) \langle \text{tr}(\bar{N} \mathbf{D}^p) \rangle \quad (52)$$

where  $\bar{U}(\bar{R})$  is the monotonically-decreasing function of  $\bar{R}$  fulfilling the conditions (see Fig. 3):

$$\tilde{U}(\tilde{R}) \begin{cases} \rightarrow \infty & \text{for } \tilde{R} = 0, \\ > 0 & \text{for } 0 < \tilde{R} < 1, \\ = 0 & \text{for } \tilde{R} = 1, \\ < 0 & \text{for } \tilde{R} > 1 \end{cases} \quad (53)$$

The incorporation of Eq. (52) furnishes the controlling function to attract the isotropic hardening stress  $\xi$  to the normal-isotropic hardening surface in the state  $\text{tr}(\tilde{\mathbf{N}}\mathbf{D}^p) > 0$ , whilst without Eq. (52) the return-mapping of  $\xi$  is required. Let the function  $\tilde{U}(\tilde{R})$  satisfying Eq. (53) be simply given by

$$\tilde{U}(\tilde{R}) = \tilde{u} \cot\left(\frac{\pi}{2}\tilde{R}\right) \quad (54)$$

where  $\tilde{u}$  is the material constant. Eq. (54) has the same form as Eq. (26) with  $R_e = 0$ .

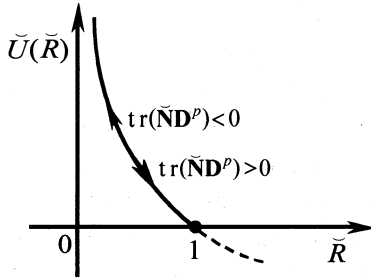


Fig. 4. Function  $\tilde{U}(\tilde{R})$  in the evolution rule of the size of sub-isotropic hardening surface.

Now, substituting Eqs. (43), (50), (51) and (52) into Eq. (48), one has

$$\begin{aligned} & \text{tr}(\tilde{\mathbf{N}}\xi_\sigma \mathbf{D}^p) - \text{tr}\{\tilde{\mathbf{N}}\tilde{\alpha}\tilde{R}^\nu \langle \text{tr}(\tilde{\mathbf{N}}\mathbf{D}^p) \rangle \tilde{\mathbf{N}}\} \\ &= \mu \left( \tilde{R} \frac{F'}{F} h(\boldsymbol{\sigma}, H_i, \tilde{R}^\nu) \langle \text{tr}(\tilde{\mathbf{N}}\mathbf{D}^p) \rangle \right) \\ & \quad + \frac{\tilde{U}(\tilde{R}) \langle \text{tr}(\tilde{\mathbf{N}}\mathbf{D}^p) \rangle}{\tilde{R}} \text{tr}(\tilde{\mathbf{N}}\xi) \end{aligned} \quad (55)$$

Assuming that the isotropic hardening stress  $\xi$  evolves when it moves the outward of the sub-isotropic hardening surface, the positive variable  $\xi_\sigma$  is given from Eq. (55) as follows:

$$\xi_\sigma = \left\{ \tilde{\alpha} \tilde{R}^\nu + \mu \left( \tilde{R} \frac{F'}{F} h(\boldsymbol{\sigma}, H_i, \tilde{R}^\nu) + \frac{\tilde{U}(\tilde{R})}{\tilde{R}} \right) \text{tr}(\tilde{\mathbf{N}}\xi) \right\} \langle \text{tr}(\tilde{\mathbf{N}}\mathbf{D}^p) \rangle \quad (56)$$

noting that the function  $h$  involves the non-negative scalar variable  $\langle \text{tr}(\tilde{\mathbf{N}}\mathbf{D}^p) \rangle$  in homogeneous degree-one. Substituting Eq. (56) into Eq. (43), the evolution rule of  $\xi$  is given as follows:

$$\dot{\xi} = \|\mathbf{D}^p\| \left\{ \tilde{\alpha} \tilde{R}^\nu + \mu \left( \tilde{R} \frac{F'}{F} h(\boldsymbol{\sigma}, H_i, \tilde{R}^\nu) + \frac{\tilde{U}(\tilde{R})}{\tilde{R}} \right) \text{tr}(\tilde{\mathbf{N}}\xi) \right\} \quad (57)$$

Accompanying with the incorporation of the cyclic stagnation of isotropic hardening, i.e. the adoption of Eq.

(50) in stead of Eq. (7)<sub>2</sub>, the rate of similarity-center in Eq. (30) and the plastic modulus in Eq. (38) are modified as follows:

$$\dot{\mathbf{s}} = \|\mathbf{D}^p\| \left\{ c \frac{\tilde{\boldsymbol{\sigma}}}{\tilde{R}} + \mathbf{a}(\boldsymbol{\sigma}, H_i) + \frac{F'}{F} h(\boldsymbol{\sigma}, H_i, \tilde{R}^\nu \langle \text{tr}(\tilde{\mathbf{N}}\tilde{\mathbf{N}}) \rangle) \hat{\mathbf{s}} \right\} \quad (58)$$

$$\begin{aligned} \bar{M}^p \equiv \text{tr} \left[ \bar{\mathbf{N}} \left\{ \frac{F'}{F} h(\boldsymbol{\sigma}, H_i, \tilde{R}^\nu \langle \text{tr}(\tilde{\mathbf{N}}\tilde{\mathbf{N}}) \rangle) \hat{\boldsymbol{\sigma}} + \mathbf{a}(\boldsymbol{\sigma}, H_i) \right. \right. \\ \left. \left. + \left\{ \frac{U}{R} + c \left( \frac{1}{R} - 1 \right) \right\} \tilde{\boldsymbol{\sigma}} \right\} \right] \end{aligned} \quad (59)$$

## 5. Material functions of metals

The material functions involved in the subloading surface model for metals formulated in the preceding sections are given as follows<sup>11</sup>:

$$f(\hat{\boldsymbol{\sigma}}) = \sqrt{\frac{3}{2}} \|\hat{\boldsymbol{\sigma}}\| \quad (60)$$

$$F(H) = F_0 [1 + h_1 \{1 - \exp(-h_2 H)\}]$$

$$\dot{H} = \sqrt{\frac{2}{3}} \tilde{R}^\nu \langle \text{tr}(\tilde{\mathbf{N}}\mathbf{D}^p) \rangle = \sqrt{\frac{2}{3}} \tilde{R}^\nu \|\mathbf{D}^p\| \langle \text{tr}(\tilde{\mathbf{N}}\tilde{\mathbf{N}}) \rangle \quad (61)$$

$$\dot{\boldsymbol{\alpha}} = \sqrt{\frac{2}{3}} a_\alpha (r_\alpha F \tilde{\mathbf{N}} - \boldsymbol{\alpha}) \|\mathbf{D}^p\| \quad (62)$$

$$f(\tilde{\xi}) = \sqrt{\frac{3}{2}} \|\tilde{\xi}\| \quad (63)$$

where  $h_1, h_2, a_\alpha, r_\alpha (< 1)$  are material constants and  $F_0$  is the initial value of  $F$ . It holds from Eqs. (57), (58), (59) and (60)-(63) that

$$\bar{\mathbf{N}} = \bar{\mathbf{N}}' = \frac{\tilde{\boldsymbol{\sigma}}'}{\|\tilde{\boldsymbol{\sigma}}'\|}, \quad \text{tr}(\bar{\mathbf{N}}\tilde{\boldsymbol{\sigma}}) = \|\tilde{\boldsymbol{\sigma}}'\|, \quad \mathbf{D}^p = \mathbf{D}^{p'} \quad (64)$$

$$\bar{\mathbf{N}} = \frac{\tilde{\xi}}{\|\tilde{\xi}\|} \quad (65)$$

$$h = \sqrt{\frac{2}{3}} \tilde{R}^\nu \left\langle \text{tr} \left( \frac{\tilde{\xi}}{\|\tilde{\xi}\|} \frac{\tilde{\boldsymbol{\sigma}}'}{\|\tilde{\boldsymbol{\sigma}}'\|} \right) \right\rangle \quad (66)$$

$$\mathbf{a} = \sqrt{\frac{2}{3}} a_\alpha (r_\alpha F \frac{\tilde{\boldsymbol{\sigma}}'}{\|\tilde{\boldsymbol{\sigma}}'\|} - \boldsymbol{\alpha}) \quad (67)$$

$$\begin{aligned} \dot{\mathbf{s}} = \|\mathbf{D}^p\| \left\{ c \frac{\tilde{\boldsymbol{\sigma}}}{\tilde{R}} + \sqrt{\frac{2}{3}} a_\alpha (r_\alpha F \frac{\tilde{\boldsymbol{\sigma}}'}{\|\tilde{\boldsymbol{\sigma}}'\|} - \boldsymbol{\alpha}) \right. \\ \left. + \sqrt{\frac{2}{3}} \frac{F'}{F} \tilde{R}^\nu \left\langle \text{tr} \left( \frac{\tilde{\xi}}{\|\tilde{\xi}\|} \frac{\tilde{\boldsymbol{\sigma}}'}{\|\tilde{\boldsymbol{\sigma}}'\|} \right) \right\rangle \hat{\mathbf{s}} \right\} \end{aligned} \quad (68)$$

$$\begin{aligned} \bar{M}^p \equiv \text{tr} \left[ \frac{\tilde{\boldsymbol{\sigma}}'}{\|\tilde{\boldsymbol{\sigma}}'\|} \left\{ \sqrt{\frac{2}{3}} \frac{F'}{F} \tilde{R}^\nu \left\langle \text{tr} \left( \frac{\tilde{\xi}}{\|\tilde{\xi}\|} \frac{\tilde{\boldsymbol{\sigma}}'}{\|\tilde{\boldsymbol{\sigma}}'\|} \right) \right\rangle \hat{\boldsymbol{\sigma}} \right. \right. \\ \left. \left. + \sqrt{\frac{2}{3}} a_\alpha (r_\alpha F \frac{\tilde{\boldsymbol{\sigma}}'}{\|\tilde{\boldsymbol{\sigma}}'\|} - \boldsymbol{\alpha}) + \left\{ \frac{U}{R} + c \left( \frac{1}{R} - 1 \right) \right\} \tilde{\boldsymbol{\sigma}} \right\} \right] \end{aligned} \quad (69)$$

$$\dot{\xi} = \|\mathbf{D}^p\| \left\{ \tilde{\alpha} \tilde{R}^\nu + \mu \left( \sqrt{\frac{2}{3}} \frac{F'}{F} \tilde{R}^{\nu+1} + \frac{\tilde{U}(\tilde{R})}{\tilde{R}} \right) \|\tilde{\xi}\| \right\}$$

$$\left\langle \frac{\text{tr}(\tilde{\sigma}' \hat{\sigma}')}{\|\tilde{\sigma}'\| \|\hat{\sigma}'\|} \right\rangle \frac{\tilde{\sigma}'}{\|\tilde{\sigma}'\|} \quad (70)$$

The subloading surface with Eq. (60) is described by the following form using Eq. (14) as follows:

$$\sqrt{\frac{3}{2}} \|\tilde{\sigma}' + R\hat{\sigma}'\| = RF(H) \quad (71)$$

i.e.

$$\text{tr}(\tilde{\sigma}' + R\hat{\sigma}')^2 = \frac{2}{3}(RF)^2 \quad (72)$$

from which  $R$  is described analytically by the following equation with the known values.

$$R = \frac{\text{tr}(\tilde{\sigma}'\hat{\sigma}') + \sqrt{\text{tr}^2(\tilde{\sigma}'\hat{\sigma}') + \left(\frac{2}{3}F^2 - \|\hat{\sigma}'\|^2\right)\|\tilde{\sigma}'\|^2}}{\frac{2}{3}F^2 - \|\hat{\sigma}'\|^2} \quad (73)$$

The value of  $R$  can be calculated analytically by Eq. (24) in the loading process ( $\mathbf{D}^p \neq \mathbf{0}$ ) but the calculation by Eq. (73) is required in the unloading process ( $\mathbf{D}^p = \mathbf{0}$ ).

## 6. Comparison with test data

The ability of the present model to reproduce the real deformation behavior of metals is examined below.

The test data for pulsating tension of 1070 steel with the axial stress from 0MPa to 830MPa is adopted for the comparison. The stress-strain curves in the test data and the simulation are depicted in Fig. 5. The values of material parameters used in the model simulation are listed in Table 1, while Eq. (28) is used for the function  $U(R)$ .

Table1. Material parameter for 1070 Steel

$F_0$	480MPa	$E$	10,500	$\nu$	0.3	$h_1$	3.2	$h_2$	10.0
$u_a$	40000	$u_b$	4	$a_\alpha$	40	$\gamma_\alpha$	0.8	$c$	100
$R_c$	0.4	$\nu$	3	$\bar{u}$	30,000	$\mu$	0.2	$\bar{\alpha}$	50,000

The stress-strain curve is predicted sufficiently well by the model. The relationship of the accumulated strain and the number of cycles is shown in Fig. 6. It is also predicted quite well.

## 7. Concluding remarks

The cyclic stagnation phenomenon of isotropic hardening observed in metals is formulated pertinently in the stress space formulation with the smooth development of isotropic hardening by incorporating the concept of the subloading surface. It will contribute to the improvement of mechanical design of machinery and structures made of metals in engineering practice.

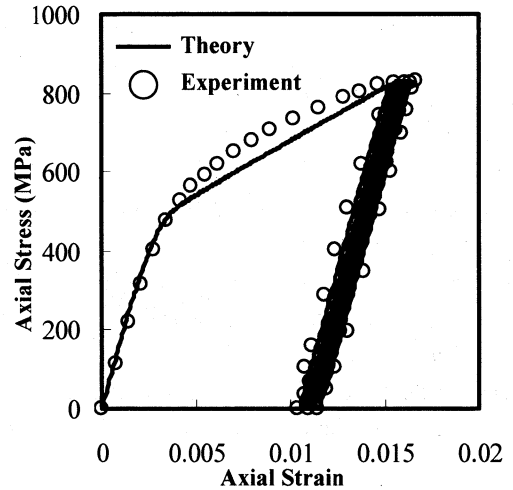


Fig.5. Relationship of stress and strain in the pulsating tension of 1070 steel.

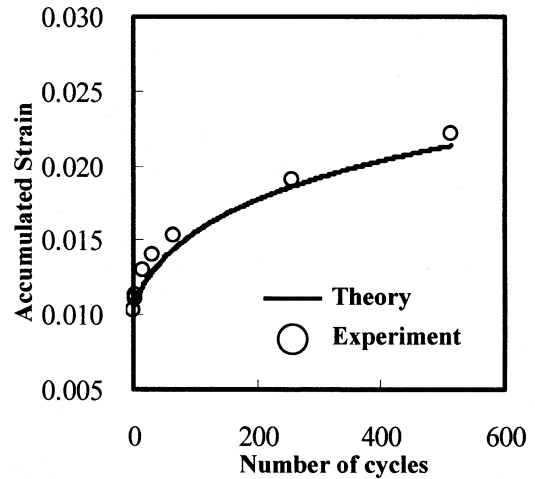


Fig.6. Relationship of number of cycles vs. accumulated strain

## References

- 1) Chaboche, J.L. and Dang-Van, K. and Cordier, G., Modelization of the Strain memory effect on the cyclic hardening of 316 stainless steel, *Trans. 5th Int. Conf. SMIRT*, Berlin, Division L., Paper No. L. 11/3., 1979.
- 2) Lemaitre, J. and Chaboche, J.-L., *Mechanics of Materials*, Cambridge Univ. Press., 1990.
- 3) Ohno, N., A constitutive model of cyclic plasticity with a non-hardening strain region, *J. Appl. Mech. (ASME)*, **49**, pp.721-727., 1982.
- 4) Ohno, N. and Kachi, Y., A constitutive model of cyclic plasticity for nonlinearly hardening materials, *J. Appl. Mech. (ASME)*, **53**, pp.395-403., 1986.
- 5) Yoshida, F. and Uemori, T., A Large-strain cyclic plasticity describing the Bauschinger effect and workhardening stagnation, *Int. J. Plasticity*, **18**, pp.661-686., 2002.
- 6) Yoshida, F. and Uemori, T., A model of large strain cyclic plasticity and its application to springback simulation, *Int. J. Mech.*

- Sci.*, **45**, pp.1687-1702., 2002.
- 7) Hashiguchi, K., Fundamental requirements and formulation of elastoplastic constitutive equations with tangential plasticity, *Int. J. Plasticity*, **9**, pp.525-549., 1993a.
  - 8) Hashiguchi, K., Mechanical requirements and structures of cyclic plasticity models, *Int. J. Plasticity*, **9**, pp.721-748., 1993b.
  - 9) Hashiguchi, K., The extended flow rule in plasticity, *Int. J. Plasticity*, **13**, pp.37-58., 1997
  - 10) Hashiguchi, K., Fundamentals in constitutive equation: Continuity and smoothness conditions and loading criterion, *Soils and Foundations*, **40**(3), pp.155-161., 2000
  - 11) Hashiguchi, K. and Yoshimaru, T., A generalized formulation of the concept of nonhardening region, *Int. J. Plasticity*, **11**, pp.347-365., 1995
  - 12) Hashiguchi, K., General corotational rate tensor and replacement of material-time derivative to corotational derivative of yield function, *Comput. Model. Eng. Sci.*, **17**(1), pp.55-62, 2007.
  - 13) Hashiguchi, K., Basic formulation of return-mapping method for subloading surface model, *Annual Research Report of Daitchi Univ.*, **20**, in press., 2008
  - 14) Hashiguchi, K., Subloading surface model in unconventional plasticity, *Int. J. Solids Struct.*, **25**, pp.917-945., 1989
  - 15) Hill, R., On the classical constitutive relations for elastic/plastic solids, *Recent Progress in Appl. Mech. (The Folke Odqvist Volume)*, John-Wiley and Sons, Chichester, pp.241-249., 1967
  - 16) Jiang, Y. and Zhang, J., Benchmark experiments and characteristic cyclic plasticity deformation, *Int. J. Plasticity*, **24**, pp.1481-1515., 1995

(Received: April 14, 2008)